Microfabricated Optical Compressive Load Sensors

Garrett D. Cole, Jack Kotovsky, Kevin L. Lin, Holly E. Petersen
Center for Micro and Nanotechnologies
Lawrence Livermore National Laboratory
Livermore, CA 94550
cole35@llnl.gov

***Abstract*—We demonstrate novel optically-addressable compressive load sensors consisting of bulk micromachined single-crystal silicon transducers integrated with fiber Bragg grating (FBG) sensing elements. These devices constitute a new class of compact optical sensors realized through the integration of mechanical components constructed via microelectromechanical systems (MEMS) fabrication technologies and strain sensitive elements based on FBGs. In this work we present experimental results for an "optical force probe" (OFP) capable of sensing compressive loading transverse to the long-axis of the fiber. Given the transduction mechanism in our design—whereby a compressive load is converted to an axial strain in the fiber—it is possible to use a standard FBG readout system to measure the imparted load. Furthermore, the sensitivity is tunable for any desired load range. Results are presented for compressive loads up to 200 psi, resulting in axial strains approaching 1000 με in the fiber.**

I. Introduction

Fiber Bragg gratings (FBGs) have been extensively studied as multipoint and multifunctional sensors for application in environmental and structural health monitoring [1]. Typically, compact FBG-based sensors are limited in operation to strain sensing in the direction parallel to the axis of the optical fiber (axial strain sensing). However, many applications require, or can benefit from, measurement of compressive loading normal to the long axis of the fiber (transverse load sensing). Transverse load measurements have previously been realized by exploiting the birefringent properties of the fiber under nonaxisymmetric loading [2]–[4]. Although this concept has proven to be successful, characterization of the sensor response becomes complicated and the ability to multiplex large numbers of sensors may be compromised. Furthermore, the sensitivity of these devices is limited by the inherent properties of the optical fiber.

In our research we seek to develop robust, small form factor, optically-addressable sensors for the measurement of compressive loading. Because these sensors are incorporated between two contacting surfaces, a major goal of this work is to minimize the thickness of the sensor in order to reduce any adverse effects on the system contact mechanics. In this application, sensors based on FBGs and micromechanical structures offer a number of advantages over existing optical sensing methodologies, including the ability to define micrometer-scale features and thus realize a compact structure, achieve tunable sensitivity through variation in the transducer geometry, and operate passively in a power-free environment. Additionally, the use of FBGs as the sensing element allows for the development of large arrays of individually addressable sensors that may be interrogated via suitable multiplexing techniques. Here, we demonstrate an optical force probe (OFP) that is capable of transforming transverse compressive loads into an axial strain in the fiber. With this design, we can leverage standard FBG interrogation techniques in order to characterize transverse loading, while simultaneously maintaining a compact sensor, with a total thickness comparable to a buffer-free silica fiber.

II. Device Design

Fig. 1 shows a three-dimensional schematic of the OFP. The structure is a hybrid sensor consisting of two distinct components: 1) the optical fiber sensor containing the internal strain sensing elements and 2) the bulk micro-machined transducer elements that convert an applied compressive force to a tensile strain in the fiber.

A. Optical Fiber Sensor

The optical fiber sensor consists of a single-mode 1550-nm fiber containing two FBGs; in this implementation one grating is exposed to the load path and thus is used for force sensing, while the second grating is included for thermal compensation. The total fiber length is 3 m and consists of an angle-polished connector, followed by 2 m of free length before the gratings. Beyond the gratings there is an optional 1-m length of fiber that can be utilized for splicing additional sensing elements, or for characterizing optical transmission through the fiber. Each of the two FBG-based strain sensors is 2 mm in length, with a physical separation distance of 1 mm. The gratings are spectrally offset by 5 nm to avoid cavity-induced resonance effects, with nominal center wavelengths of 1550 nm and 1555 nm. The full width at half maximum (FWHM) of the grating stop-band is measured to be 0.97 nm. An approximately 2 cm section where the gratings are written is left uncoated, exposing a bare silica surface for integration of the transducer elements.

This work was performed under the auspices of the U. S. Department of Energy (DOE) by the University of California, Lawrence Livermore National Laboratory (LLNL) under Contract no. W 7405 Eng 48.

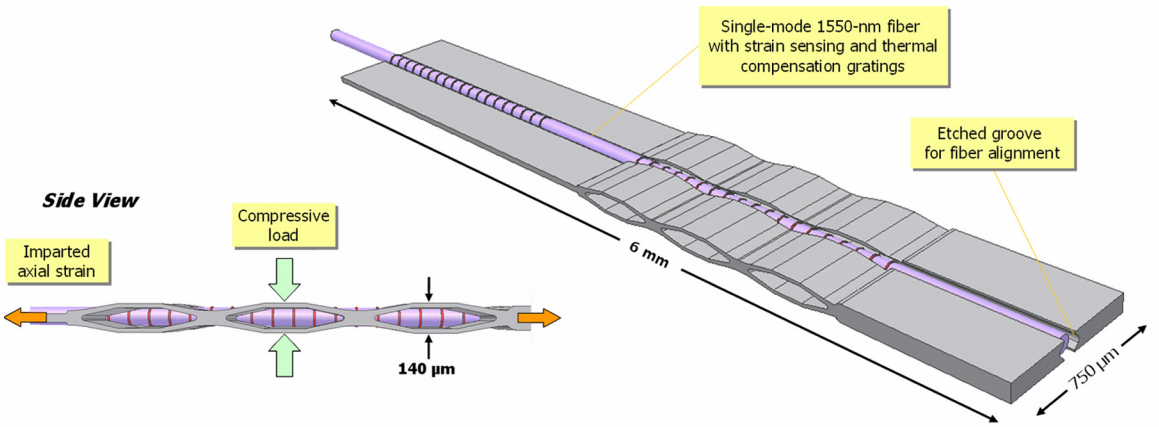

Figure 1. Three-dimensional schematic of the hybrid silicon / FBG optical compressive load sensor. The structure consists of bulk micromachined single-crystal silicon transducers integrated with a single-mode 1550-nm optical fiber containing a pair of FBG-based strain sensing elements. In this structure the silicon transducers convert an applied compressive load to an axial strain in the fiber. There are two gratings in each force probe; one strain-sensitive grating that is clamped on either end of the flared silicon structure highlighted above (in side view), while the second grating is used for thermal compensation.

B. Micromachined Transducer Elements

The transducer elements consist of single-crystal silicon (SCS) mechanical elements that are micromachined to define geometry for fiber alignment as well as mechanical transduction. Along the length of these components a semicircular groove is defined for fiber alignment; this feature is fabricated via an isotropic plasma etching process described in the following section. As shown in Fig. 1, mechanical transduction is realized through the incorporation of flexures that extend beyond the outer-diameter of the optical fiber sensor. In this design, under an applied external load (in an orientation perpendicular to the long-axis of the fiber), the flexures are compressed, resulting in an extension of the silicon transducer and optical fiber sensor.

A finite element simulation of the axial strain response of the OFP to a compressive load is shown in Fig. 2. Because the fiber is bonded to the transducer at either end of the open flexure structure, the compressive load results in a tensile strain imparted along the long-axis of the fiber, which increases the periodicity of the FBG and leads to a red-shift in the peak reflectance. In this simulation, the application of 200 psi results in a uniform axial strain of 773 με in the fiber. By varying the geometry of the flexures, the imparted tensile strain in the fiber—and corresponding wavelength shift of the FBGs—can be tuned to the desired sensitivity level. Finally, because the compressive load is transformed into an axial strain in the FBG, standard readout hardware may be utilized for the characterization of transverse loading.

III. FABRICATION

A. Bulk Micromachining of the SCS Transducers

The silicon transducer elements are fabricated in a batch fashion out of a nominally 375-µm thick ‹100› oriented SCS wafer that is double-side polished. For the first portion of the process, a groove is defined in the surface of the silicon in order to constrain the location of the optical fiber along the transducer element. For the fiber alignment groove we have developed a process to achieve a near ideal semicircular cross-section, allowing for intimate contact with the stripped fiber, as indicated in Fig. 3. The isotropic nature of this etch results in the formation of a semicircular cross-section from rectangular trench openings in a standard positive photoresist mask. After stripping the resist, the aspect ratio of the groove may be tuned with further SF_6 etching; in this case lateral features etch rapidly (4.09 µm/min), while the vertical direction shows minimal change in height (decreasing at 0.31 µm/min) as all exposed surfaces etch at a roughly constant rate. Following the definition of the fiber-groove, the wafer is mounted groove-side down to a quartz carrier using a high temperature mounting adhesive. The use of the quartz handle allows for backside alignment and also constrains the released components to remain in place at the termination of the through-wafer etch process.

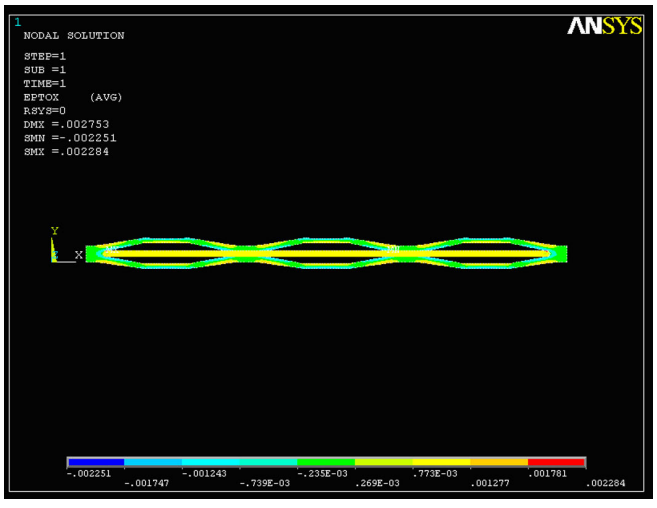

Figure 2. Finite element simulation of the OFP strain response. The device modeled here has three sets of flextures, with a thickness of 40 µm. At 200 psi, 773 με is imparted to the optical fiber sensor.

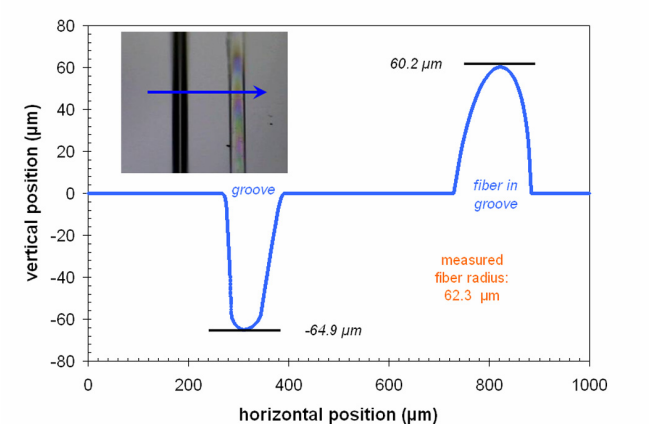

Figure 3. Profilometer measurement (along indicated path) of the fiber-constraint grooves. Intimate contact between the bare-silica fiber and silicon is indicated by the appearance of Newton's Rings in the inset image.

Subsequent to the groove etch and temporary mounting process, the transducer geometry is patterned with positive photoresist on the exposed surface of the silicon wafer. These structures are registered to the groove pattern via a backside alignment process through the optically-transparent quartz handle wafer. The transducer geometry is then extruded through the full thickness of the SCS wafer using a deep reactive ion etch system (DRIE) with a standard cyclic silicon etching process (SF_6 as the etchant, alternating with C_4F_8 for passivation). With the completion of the through-wafer etch process, the individual transducer elements are released from the quartz carrier by soaking in heated photoresist stripper. An example of a free-standing microfabricated SCS transducer can be seen in Fig. 4 below.

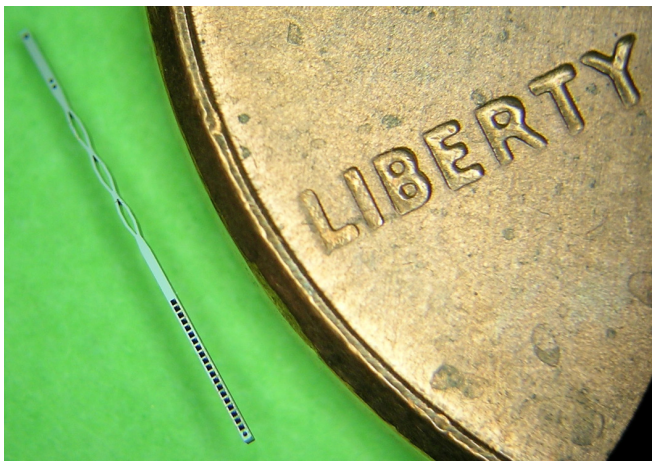

Figure 4. A microfabricated SCS transducer element after releasing from the quartz handle wafer. In this case the fiber alignment groove is on the opposite side of the structure. The component is pictured next to a US penny in order to demonstrate the scale of the part.

B. *Assembly of the Optical Force Probe*

Joining of the optical fiber sensor and silicon transducers takes place in a custom designed alignment station. In this setup the fiber is stretched between two grips to a controlled pre-tension value (monitored real-time with a commercial Micron Optics readout system). A multi-axis positioner (x, y, z, θ) is used to align the silicon transducer with the fiber and bring it into contact for bonding. For ease of handling, the silicon components are temporarily mounted to a glass cover-slip using a high temperature wax. In order to accurately locate the grating position within the fiber, we utilize a localized heating technique similar to that described in [5]. For this process we employ a tungsten microprobe mounted on a thermoelectric heating element, and translated along the axis of the fiber with a micropositioner. By scanning the heated probe tip across the surface of the fiber, the center of the grating may be found. An example of the spectral shift induced by this process is included as Fig. 5.

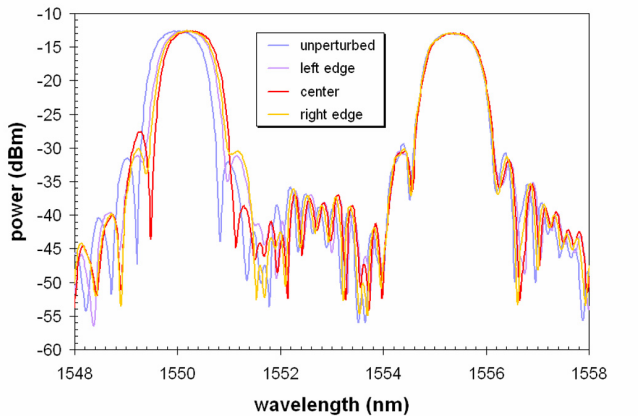

Figure 5. Spectral response of the optical fiber sensor recorded during the grating alignment procedure; note that the probe is in contact with the 1550-nm FBG, while the 1555-nm FBG remains unaffected. The maximum spectral shift occurs when the probe is aligned with the grating center.

Using the localized heating technique we estimate that it is possible to achieve an alignment accuracy on the order of 250 µm. As compared with optical location methods such as the side scattering technique [6], the heated probe method is comparably simpler and also allows for grating imaging through opaque media, such as metal clad optical fibers. Bonding of the Si components and optical fiber relies on the use of a dual-cure (UV/thermal) epoxy that is applied to the silicon transducer using a dip-pen approach. In this procedure the epoxy is applied to the silicon element by using a section of bare silica optical fiber loaded with a small bead of uncured epoxy. Application along the transducer is realized by wetting the bead of epoxy into the groove and then translating the fiber with a micropositioner. This system allows for accurate and repeatable application of small volumes of epoxy to the desired locations on the transducer elements. For the OFP, epoxy is applied within the thermal compensation section, and additionally, at either end of the flexure structure.

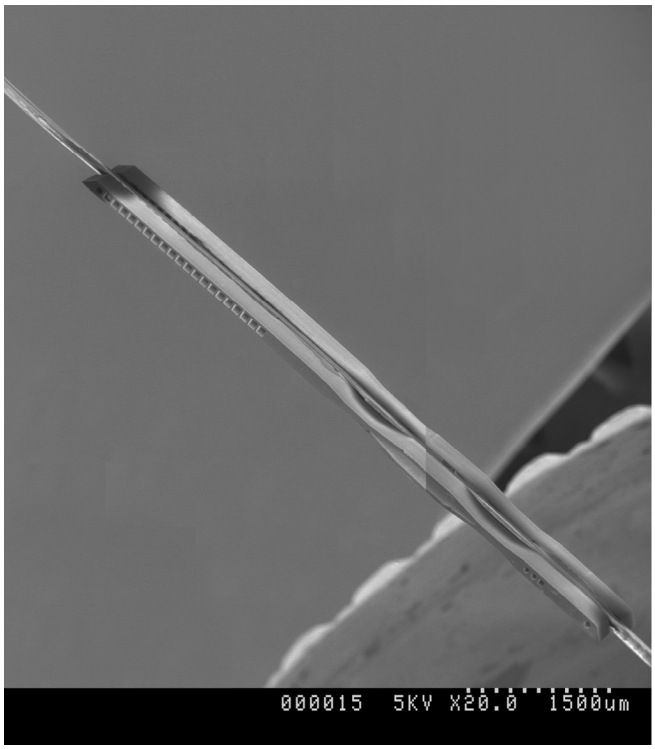

Figure 6. Scanning electron micrograph of a completed optical force probe. This view was generated by stitching together two separate images.

With the gratings located and the epoxy application completed, the fiber is brought into intimate contact with the silicon groove in the alignment station and an initial UV cure is performed, followed by a final thermal cure at 120º C. We have found that O_2 plasma exposure immediately prior to the epoxy application enhances the adhesive strength of the bond. After fully curing the epoxy, the transducer is removed from its temporary handle by rinsing in acetone followed by isopropanol. To complete the symmetric OFP structures (incorporating two micromechanical transducers surrounding the fiber) the assembly process is repeated with the second transducer visually aligned with the first. A scanning electron micrograph of a completed force probe is presented in Fig. 6.

IV. Characterization

Testing of the sensor response makes use of an Instron materials characterization system configured for compressive loading. This system utilizes two 2-inch diameter stainless steel compression anvils, each lined with 0.5 mm latex. Because of the small thickness of the sensor when compared with the thickness of the compliant loading surfaces (140 µm thick OFP compared with 1 mm total latex thickness), the presence of the sensor in this configuration does not perturb the load path and the force is assumed to be uniform across the full area of the compression anvils. This is one of the major advantages of the microfabricated OFP—due to the extreme slenderness of the structure it is possible to achieve a near mechanical invisibility. During testing, the peak reflectivity of the grating is recorded with a commercial Micron Optics interrogation system. Peak tracking is used to monitor the shift in Bragg wavelength as a function of the applied compressive load. Data from a single-transducer sensor is presented in Fig. 7. In this experiment the sensor was subjected to a single-cycle compressive load resulting in an applied pressure varying from 40–180 psi. The sensor exhibits a repeatable linear response in the range of 60–180 psi with a sensitivity of 6.52 pm/psi. Assuming a strain induced peak shift of 1.21 pm/µε at 1550 nm, this converts to an axial strain transduction of 5.38 µε/psi for this geometry.

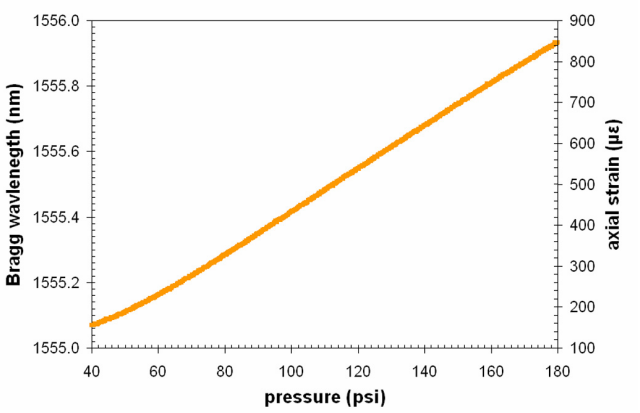

Figure 7. Typical response of the single-tansducer OFP to a single loading cycle up to 180 psi. The device exhibits a linear change in the Bragg wavelength of the grating over a range of approximately 120 psi (from 60–180 psi). In this design (the same as that presented in the finite element model in Fig. 2), the sensitivity of the structure is 6.53 pm/psi (5.38 µε/psi).

V. Conclusion

We have demonstrated a unique class of optical compressive load sensors based on the integration of microfabricated mechanical transducers and FBG-based optical fiber sensors. Preliminary results from these devices are very encouraging, with a sensitivity of 6.52 pm/psi (converting to an axial strain of 5.38 µε/psi) resulting in a total strain of 866 µε at 180 psi.

References

[1] E. Udd, "Overview of Fiber Optic Sensors," in *Fiber Optic Sensors*, F. Wu, S. Yin, Eds. New York: Marcel Dekker, 2002, pp. 1–40.

[2] Y. Liu, L. Zhang, I. Bennion, "Fibre optic load sensors with high transverse strain sensitivity based on long-period gratings in B/Ge co-doped fibre," *Electron. Lett.*, vol. 35, April 1999, pp. 661–663.

[3] M. LeBlanc, S. T. Vohra, T. E. Tsai, E. J. Friebele, "Transverse load sensing by use of pi-phase-shifted fiber Bragg gratings," *Opt. Lett.*, vol. 24, August 1999, pp. 1091–1093.

[4] C. Caucheteur, S. Bette, R. Garcia-Olcina, M. Wuilpart, S. Sales, J. Capmany, P. Mégret, "Transverse strain measurements using the birefringence effect in fiber Bragg gratings," *IEEE Photonic. Tech. L.*, vol. 19, July 2007, pp. 966–968.

[5] Y. N. Roussel, S. Magne, C. Martinez, P. Ferdinand, "Measurement of index modulation along fiber Bragg gratings by side scattering and local heating techniques," *Opt. Fiber Technol*, vol. 5, January 1999, pp. 119–132.

[6] P. A. Krug, R. Stolte, R. Ulrich, "Measurement of index modulation along an optical fiber Bragg grating,'' *Opt. Lett*., vol. 20, September 1995, pp. 1767–1769.